

1 **AICAR and Compound C negatively modulate HCC-induced primary human**
2 **hepatic stellate cell activation in vitro**

3 Katrin Böttcher ^{1,2}, Lisa Longato ¹, Giusi Marrone ¹, Giuseppe Mazza ¹, Leo Ghemtio ³,
4 Andrew Hall ^{2,4}, Tu Vinh Luong ⁴, Stefano Caruso ⁵, Benoit Viollet ⁶, Jessica Zucman-Rossi ^{5,7},
5 Massimo Pinzani ^{1,2}, Krista Rombouts ^{1*}

6

7 ¹Regenerative Medicine and Fibrosis Group, Institute for Liver and Digestive Health,
8 University College London, Royal Free Campus, NW3 2PF London, UK; ²Sheila Sherlock Liver
9 Centre, Royal Free Hospital, NW3 2PF London, UK; ³Drug Research Program, Division of
10 Pharmaceutical Biosciences, Faculty of Pharmacy, University of Helsinki, FI-00014, Helsinki,
11 Finland; ⁴Royal Free Hospital, Department of Cellular Pathology, London, UK; ⁵Centre de
12 Recherche des Cordeliers, INSERM, Sorbonne Université, Université de Paris, Université
13 Paris 13, Functional Genomics of Solid Tumors laboratory, F-75006 Paris, France; ⁶Université
14 de Paris, Institut Cochin, CNRS, INSERM, Paris, F-75014 Paris, France; ⁷Hôpital Européen
15 Georges Pompidou, F-75015, Assistance Publique-Hôpitaux de Paris, Paris, France.

16

17 **Figure number:** 5 Figures, 6 supplementary figures

18 **Word count:** 9366

19 **Running title:** HCC-stellate cells paracrine cross-talk

20

21 **Key words:** Hepatocellular carcinoma (HCC), tumour-stromal interactions, liver fibrosis,
22 adenosine monophosphate-activated kinase (AMPK), Hepatic Stellate Cells (HSC), AICAR,
23 Compound C, TCGA, LICA-FR

24

25 ***Contact information corresponding author:**

26 Professor Krista Rombouts, PhD

27 UCL Institute for Liver and Digestive Health, Royal Free Hospital

28 Rowland Hill Street

29 London NW3 2PF

30 United Kingdom

31 Telephone: +44 (0)20 80168372

32 E-mail: k.rombouts@ucl.ac.uk

33

34 **List of abbreviations:**

35 **hHSC** human hepatic stellate cell

36 **AMPK** adenosine monophosphate-activated kinase

37 **AMPK α 1** AMP-activated protein kinase subunit α 1

38 **AMPK α 2** AMP-activated protein kinase subunit α 2

39 **p-AMPK** phosphorylated AMPK

40 **AMPK α 1 α 2-null** AMP-activated protein kinase subunit α 1 α 2 – deficient

41 **MEF** mouse embryonic fibroblasts

42 **Wt** wild type

43 **BrdU** 5-bromo-2-deoxyuridine

44 **MTS** 3-(4,5-dimethylthiazol-2-yl)-5-(3-carboxymethoxyphenyl)-2-(4-sulfophenyl)-2H-tetrazolium inner salt

46 **qPCR** quantitative polymerase chain reaction

47 **MEF** mouse embryo fibroblasts

48 **CM** Complete medium

49 **SFM** Serum free medium

50 **4E-BP1** eukaryotic translation initiation factor 4E-binding protein 1

51 **AICAR** 5-aminoimidazole-4-carboxamide-1- β -d-ribofuranosid

52 **CC** Compound C

53 **BrdU** bromodeoxyuridine

54 **CCL** CC motif chemokine ligand

55 **ECM** extracellular matrix

56 **ELISA** enzyme linked immunosorbent assay

57 **GAPDH** glyceraldehyde 3-phosphate dehydrogenase

58 **IL** interleukin

59 **LKB1** liver kinase B1, also called STK11 serine/threonine kinase 11

60 **LOX** lysyl oxidase

61 **mTOR** mammalian target of rapamycin

62 **TIMP** tissue inhibitor of matrix metalloproteinase

63 **GLUL** Glutamate-Ammonia Ligase

64 **LGR5** Leucine Rich Repeat Containing G Protein-Coupled Receptor 5

65 **LAMA3** Laminin Subunit Alpha 3

66

67 **Financial support** : This research was funded by grants from the NIHR UCLH BRC (M.P. and
 68 K.R.), the Royal Free Charity (M.P.). L.G. gratefully acknowledges the support of The Drug
 69 Discovery and Chemical Biology – Biocenter Finland and The CSC - IT Center for Science Ltd.
 70 (Helsinki, Finland) for organizing computational resources. J.Z-R. group was supported by
 71 INSERM, Ligue Nationale contre le Cancer (Equipe Labellisée), Labex Oncolmunology
 72 (investissement d'avenir), grant IREB, Coup d'Elan de la Fondation Bettencourt-Schueller,
 73 the SIRIC CARPEM, Raymond Rosen Award from the Fondation pour le Recherche Médicale,

74 Prix René and Andrée Duquesne - Comité de Paris Ligue Contre le Cancer and Fondation
75 Mérieux. S.C. was supported by a funding from Labex Oncolmunology and CARPEM. Giusi
76 Marrone received funding through a post-doctoral Fellowship by the European Association
77 for the Study of the Liver (EASL). K.B. received funding through a Physician-Scientist
78 Fellowship by the European Association for the Study of the Liver (EASL).

79

80 **Conflict of interest**

81 “The funders had no role in the design of the study; in the collection, analyses, or
82 interpretation of data; in the writing of the manuscript, or in the decision to publish the
83 results”. The authors declare no conflict of interest with regards to the present manuscript.
84 Giuseppe Mazza, and L.L. are now full time employees at Engitix Ltd., and Giuseppe Mazza,
85 L.L., M.P., and K.R. own shares in Engitix Therapeutics Ltd., M.P., T.V.L, A.H. and K.R. receive
86 consultancies from Engitix Ltd.

87

88 **Authors contributions:**

89 KR designed the study; KB conducted experiments; KR performed HSC isolation; GM, KB,
90 and LL performed HSC culture; AH, TVL performed ICH, LG and SC performed bioinformatics;
91 BV provided MEFs; JZR provided HCC cell lines; KB, KR and MP analysed data; KB and KR
92 wrote the manuscript; KR and MP critically revised the manuscript; all authors have edited
93 the paper and approved the final manuscript.

94

95 **Acknowledgments:** The results shown here are part based upon data generated by the
96 TCGA <https://www.cancer.gov/tcga> and <https://icgcportal.genomics.cn/projects/LICA-FR>.
97 We thank Prof Brian Davidson, Prof Barry Fuller and Dr Amir Gander (Tissue Access for
98 Patient Benefit) and the NHSBT, for providing tissue samples for our research.

99

100

101 Abstract

102 Tumour stroma and microenvironment have been shown to affect hepatocellular carcinoma
103 (HCC) growth, with activated hepatic stellate cells (HSC) as a major contributor in this
104 process. Recent evidence suggests that the energy sensor adenosine monophosphate-
105 activated kinase (AMPK) may mediate a series of essential processes during carcinogenesis
106 and HCC progression. Here, we investigated the effect of different HCC cell lines with known
107 *TP53* or *CTNBB1* mutations on primary human HSC activation, proliferation and AMPK
108 activation. We show that conditioned media obtained from multiple HCC cell lines
109 differently modulate human hHSC proliferation and hHSC AMPK activity in a paracrine
110 manner. Pharmacological treatment of hHSC with AICAR and Compound C inhibited the
111 HCC-induced proliferation/activation of hHSC through AMPK-dependent and AMPK-
112 independent mechanisms, which was further confirmed using mouse embryonic fibroblasts
113 (MEFs) deficient of both catalytic AMPK α isoforms (AMPK ^{α 1/ α 2-/-}) and wild type (wt) MEF.
114 Both compounds induced S-phase cell-cycle arrest and, in addition, AICAR inhibited the
115 mTORC1 pathway by inhibiting phosphorylation of 4E-BP1 and S6 in hHSC and wt MEF.
116 Datamining of the Cancer Genome Atlas (TCGA) and the Liver Cancer (LICA-FR) showed that
117 AMPK α 1 (*PRKAA1*) and AMPK α 2 (*PRKAA2*) expression differed depending on the mutation
118 (*TP53* or *CTNNB1*), tumour grading and G1-G6 classification, reflecting the heterogeneity in
119 human HCC. Overall, we provide evidence that AMPK modulating pharmacological agents
120 negatively modulate HCC-induced hHSC activation and may therefore provide a novel
121 approach to target the mutual, tumour-promoting interactions between hHSC and HCC.

122

123

124

125

126

127

128

129

130

131

132 NEW & NOTEWORTHY

133 HCC is marked by genetic heterogeneity and activated hepatic stellate cells (HSC) are
134 considered key players during HCC development. The paracrine effect of different HCC cell
135 lines on the activation of primary hHSC was accompanied by differential AMPK activation
136 depending on the HCC line used. Pharmacological treatment inhibited the HCC-induced
137 hHSC activation through AMPK-dependent and AMPK-independent mechanisms. This
138 heterogenic effect on HCC-induced AMPK activation was confirmed by datamining TCGA
139 and LICA-FR databases.

140

141 **Introduction**

142 Hepatocellular carcinoma (HCC) is the most common primary liver tumour and one of the
143 leading causes for cancer deaths (18). More than 80% of HCC develop on the background of
144 liver cirrhosis following long-standing liver injury most commonly caused by chronic
145 infection with hepatitis B or C viruses, excess alcohol consumption, or non-alcoholic
146 steatohepatitis (37). In these clinical conditions, chronic liver damage is characterized by the
147 activation of hepatic stellate cells (HSC), which represent the main cellular effectors of
148 hepatic fibrosis and consequent progression to liver cirrhosis (42). Activation of HSC is
149 characterized by the transition from a quiescent pericyte to a myofibroblast-like cell with
150 increased proliferation, migration, contraction and expression of pro-fibrogenic factors, pro-
151 inflammatory cytokines and extracellular matrix (ECM) components, resulting in the
152 formation of a scar tissue (48, 57). There is growing evidence that the tumour
153 microenvironment, in particular the bidirectional cross-talk between HCC and HSC, is a
154 crucial factor for HCC onset and progression (10) as activated HSC enhance HCC cell
155 proliferation, migration and tumour growth (2) by fostering the pro-inflammatory and pro-
156 angiogenic microenvironment of the tumour (16).

157 The energy-sensing enzyme adenosine monophosphate-activated kinase (AMPK) is a highly
158 sensitive safeguard that responds to changes in ATP production and promotes catabolic
159 pathways while inhibiting anabolic pathways when activated (41). Importantly, AMPK has
160 been implicated in tumour development and progression as AMPK regulates the cell cycle
161 by stabilizing p53 and p27 (32, 52). Thus, AMPK inhibits cell growth, metabolism and
162 proliferation through inhibition of the mTOR pathway (20). Further evidence for AMPK as a
163 tumour suppressor is originating from clinical and experimental data showing that
164 pharmacological AMPK modulators inhibit cancer development and progression (34, 53).
165 Indeed, the incidence of HCC is lower in diabetic patients treated with metformin which
166 induces AMPK activity (13). Metformin has also been shown to inhibit angiogenesis in an
167 HCC – HSC cell line *in vitro* co-culture model, supporting an inhibitory role for AMPK in
168 tumour-stromal interactions (45). In addition, AICAR, another well-established AMPK
169 activator, suppresses HCC cell proliferation and inhibits tumour growth in murine HCC models
170 *in vivo* (14). Of note, pharmacological activation of AMPK has been shown to reverse HSC
171 activation *in vitro* and AICAR and metformin inhibits PDGF-induced HSC proliferation (1, 9).

172 Nevertheless, there is limited evidence for a role of AMPK in the tumour-stromal interaction
173 between HCC cells and primary human HSC, as well as for the possible working mechanisms
174 of AMPK in such cross-talk. Accordingly, the present study was designed to provide further
175 evidence on the involvement of this pathway in the cross-talk between HCC and its stroma.
176 As HCC is known to be a highly heterogeneous cancer (8, 17) several HCC cell lines with
177 different types of mutations were investigated in this study.

178 The results of the study show that activation of AMPK is involved in HCC tumour-stromal
179 interaction and suggests AMPK as a potential target for novel treatments for the overall
180 stromal derangement typical of chronic liver disease and the associated development of
181 HCC.

182

183 **Material and Methods**

184

185 **Patients and tumours**

186 The expression levels of AMPK α 1 (*PRKAA1*) and AMPK α 2 (*PRKAA2*) were assessed by RNA-
187 seq in two independent datasets, including 160 HCC samples from LICA-FR cohort previously
188 described, and 339 HCC samples from the TCGA (The Cancer Genome Atlas) cohort. Patients
189 with co-occurring *TP53* and *CTNNB1* mutations were excluded from the analysis. At least
190 two liver pathologists used multiple slides of the same tumour to establish the Edmondson-
191 Steiner grades in both cohorts, as previously described (23). Furthermore, the expression of
192 AMPK α 1 (*PRKAA1*) and AMPK α 2 (*PRKAA2*) was investigated in relation to the G1-G6
193 classification (5). Detailed clinical characteristics for both datasets are provided in
194 Supplemental Table S1 (supplemental material for this article is available online at
195 <https://figshare.com/s/6953f837617d681232d7> and DOI 10.5522/04/12562631).

196

197 **Immunohistochemistry**

198 Immunostaining of AMPK α 1 subunit was performed as previously described on formalin
199 fixed paraffin-embedded human liver sections from histologically normal tissue retrieved
200 from sites remote to colorectal liver metastasis, cirrhotic liver without HCC and HCC in the
201 context of a cirrhotic liver obtained from the Royal Free Hospital histopathology archives
202 (ethics 07/Q0501/50) (39). Liver sections were de-paraffinized and hydrated through

203 xylenes and ethanol. Antigen retrieval was achieved by microwaving the section at 640 W
204 for 20 minutes in 1L of pH9.0 Tris EDTA buffer. The slides were soaked in TBS with 0.04%
205 Tween-20 (Sigma) for 5 minutes and blocked for endogenous peroxidase and non-specific
206 binding of secondary antibodies using reagents from the Novolink kit (Leica), 5 minutes
207 each. AMPK α 1 antibody (Abcam ab32047) was incubated for 1 hour at room temperature.
208 The primary antibody was then detected using Novolink kit reagents, post primary 30
209 minutes, polymer 30 minutes and DAB 5 minutes. The slides were then counterstained with
210 Mayer's haematoxylin. All sections were dehydrated, cleared in xylene, mounted with DPX
211 (Leica biosystems), and observed using a Zeiss Axioskop 40. Images were captured with an
212 Axiocam Icc5 using Zeiss Axiovision (version 4.8.2).

213

214 **Human HSC isolation**

215 Human HSC (hHSC) were isolated from wedge sections of human liver tissue, obtained from
216 patients undergoing liver surgery at the Royal Free Hospital after giving informed consent
217 (NC2015.020 (B-ERC-RF)), as described before (38, 49). Briefly, 10g of total human liver
218 tissue was digested with 0.01% Collagenase type IV (Sigma Aldrich), 0.05% Pronase
219 (Calbiochem) and 0.001% DNase I (Sigma Aldrich). The homogenate was filtered through a
220 100 μ m cell strainer (BD Falcon) and the flow-through was centrifuged at 50 x g for 2
221 minutes at 4°C to remove hepatocytes. After washing the supernatant, gradient
222 centrifugation was performed at 1400 x g for 17 minutes using a 11.5% Optiprep gradient
223 (Sigma Aldrich). Finally, the interface was collected and washed. The obtained hHSC were
224 cultured in Iscove's Modified Dulbecco's Medium supplemented with 20% foetal bovine
225 serum (FBS), 2 mM/l glutamine, nonessential amino acids 1x, 1.0 mM/l sodium pyruvate,
226 antibiotic-antimycotic 1x (all GIBCO), referred to as complete HSC medium hereinafter.
227 Experiments were performed on cells between passage 3 and 8 employing at least three
228 different cell preparations/donors for all experiments.

229

230 **Cell lines**

231 HepG2 and PLC/PRF/5 were purchased from American Type Culture Collection (ATCC®) and
232 cultured in Minimum Essential Medium α supplemented with 10% FBS, nonessential amino
233 acids 1x, 1.0 mM/l sodium pyruvate, Antibiotic-Antimycotic 1x. HCC cells lines SNU398,
234 Mahlavu, Huh-6 and Huh-7 cells were kindly provided by Prof Jessica Zucman-Rossi and

235 identity of the cell lines was confirmed by sequencing (11). Cells were cultured in Dulbecco's
236 modified Eagle Medium, supplemented with 10% FBS and Penicillin/Streptomycin. All cell
237 cultures are frequently analysed for mycoplasma using an in-house qPCR assay as previously
238 described (58).

239 **Mouse embryonic fibroblasts**

240 Simian virus 40 large T antigen immortalized mouse embryonic fibroblasts (MEFs) were
241 kindly provided by Dr Benoit Viollet. AMPK α 1/ α 2^{-/-} and wt MEFs were obtained from 10.5
242 day postcoitum embryos, the genotype was confirmed by PCR and immunoblot analysis.
243 MEFs from the second or third culture passage were immortalized by introducing the SV 40
244 large T antigen using the pSV-Ori- vector (30). MEFs were cultured in Dulbecco's Modified
245 Eagle Medium supplemented with 10% FBS, 1mM sodium pyruvate and Antibiotic-
246 Antimycotic 1x (all GIBCO).

247

248 **Preparation of conditioned medium**

249 To obtain conditioned medium 3 x 10⁶ HepG2 or PLC/PRF/5 cells, or 0.6 x 10⁶ hHSC were
250 cultured in a cell culture dish (100 x 22mm) in complete HCC or hHSC medium. After 24h,
251 cells were washed twice with HBSS and incubated in serum-free medium for 48h.
252 Conditioned medium was collected and centrifuged at 247 x g, 7 min, 21°C. The supernatant
253 was used immediately, or stored at -20°C, until used for experiments.

254

255 **Treatment of cells**

256 *Treatment of hHSC with conditioned medium of HepG2 or PLC/PRF/5 cells*

257 Human HSC were plated on a cell culture dish (0.3 x 10⁶/6 well or 0.006 x 10⁶/ 96 well) in
258 complete HSC medium. After 24 hours, cells were washed with HBSS (Gibco) and serum-
259 starved for 24 hours. Subsequently cells were treated with conditioned medium of HepG2
260 or PLC/PRF/5 cells for 24 hours.

261 *Treatment of HepG2 and PLC/PRF/5 cells with conditioned medium of hHSC*

262 HepG2 or PLC/PRF/5 cells were plated on a cell culture dish (0.006 x 10⁶/ 96 well) in
263 complete HCC medium. After 24 hours, cells were washed with HBSS (Gibco) and serum-
264 starved for 24 hours, and cells were treated with conditioned medium of different primary
265 hHSC preparations subsequently.

266 *Treatment of cells with pharmacological compounds*

267 Human HSC were treated with different concentrations of AICAR (0.25-4mM) reconstituted
268 in water, or Compound C (2.5-40 μ M) reconstituted to 10mM in DMSO. Cells were plated in
269 complete medium and serum-starved for 24 hours prior to treatment.

270

271 **BrdU incorporation assay**

272 Cell proliferation was quantified by BrdU Cell Proliferation ELISA kit (Roche) and as
273 described before (4, 38). Human HSC (10^3) were plated in complete medium in a 96 well
274 plate in quadruplicates. Cells were washed and serum-starved for 24 hours prior to
275 treatment. BrdU labelling solution was added in parallel with treatment, BrdU ELISA was
276 developed according to the manufacturer's protocol after 24 hours treatment and
277 absorbance was detected with Fluostar Omega Plate Reader (BMG labtech).

278

279 **MTS assay**

280 To determine metabolic activity of cells, CellTiter 96[®] Aqueous One Solution Cell
281 Proliferation Assay kit (Promega) was used according to the manufacturer's protocol and as
282 previously described (39). Briefly, hHSC (10^3) were plated in complete medium in a 96 well
283 plate in quadruplicates and were cultured and treated as described above. Following 24
284 hours treatment, MTS was added for 2 hours and absorbance was measured with Fluostar
285 Omega Plate Reader (BMG labtech).

286

287 **Cell cycle analysis**

288 For cell cycle analysis, 0.3×10^6 HSC were plated on a 6 well plate in complete medium.
289 After 24 hours, cells were washed and cultured in serum-free medium for 24 hours,
290 followed by treatment. Cells were trypsinised after 24 hours of treatment, washed and fixed
291 with ice-cold 70% ethanol, for 30 minutes at 4°C. Cells were washed twice before incubation
292 with propidium iodide (50 μ g/ml, Promega) for 10 minutes at room temperature. Propidium
293 iodide accumulation was analysed with BD LSR Fortessa (5L SORP) using BD FACSDiva
294 software (version 6.2) and analysed with FlowJo version 10.0.

295

296 **Cell death enzyme linked immunosorbent assay (ELISA)**

297 To analyse apoptosis and necrosis in hHSC, Cell Death Detection ELISAPlus (Roche) was used
298 according to the manufacturer's protocol. Cells were treated in triplicates. Following 24

299 hours treatment, supernatants were removed and cells were lysed. Nucleosomes were
300 quantified in cell lysates (apoptosis) and supernatants (necrosis) photometrically.
301 Absorbance at 420nm was measured with Fluostar Omega Plate Reader (BMG labtech).

302

303 **Western blot analysis**

304 Protein isolation and western blot analysis was performed as previously described (4, 38,
305 39). To obtain total protein cell lysates, cells were washed and lysed with radio
306 immunoprecipitation assay (RIPA) buffer (20 mM Tris-HCl pH 7.6, 150mM NaCl, 5mM EDTA,
307 1% NP-40 (nonyl phenoxypolyethoxyethanol), 1mM phenylmethylsulfonyl fluoride (PMSF),
308 1X Protease Inhibitors Mix, 1mM Na₃VO₄ and 1mM NaF). Cell lysates were sonicated with
309 the “Ultrasonic Processor” (Sonics, Vibra Cell). Protein quantification was carried out using
310 Micro BCATM Protein Assay Kit, (Thermo Scientific) according to the manufacturer’s
311 protocol. SDS gel electrophoresis was performed with 25µg of protein lysate were loaded on
312 10% or 12% acrylamide gels. Primary antibodies were incubated overnight at 4°C or for 1
313 hour at room temperature. After washing, specific horseradish peroxidase coupled
314 secondary antibodies were applied for 1 hour at room temperature and SuperSignal® West
315 Pico Chemiluminescent Substrate (Thermo Scientific) was used to develop signals. For
316 following antibody incubations, antibodies were stripped with Restore™ PLUS Western
317 Blot Stripping Buffer (Thermo Scientific). To verify equal loading of samples, expression of
318 the house-keeping proteins β-actin or tubulin was detected. All primary and secondary
319 antibodies are listed in supplemental table S2 and antibody specificity was validated by
320 performing western blot analysis.

321

322 **Quantitative real-time PCR (qPCR)**

323 RNA was isolated from hHSC using RNeasy mini Kit (Qiagen) according to the manufacturer’s
324 protocol and as previously described (4, 38, 39). Purity and RNA concentration were
325 measured with Nanodrop spectrophotometer (Thermo Scientific) and cDNA was synthesized
326 with MultiScribe reverse transcriptase, random primers, deoxyribose nucleoside
327 triphosphate (dNTP) mix and RNase inhibitor (all Applied Biosystems). Gene expression was
328 measured via quantitative real time PCR (qPCR) using Taqman gene assays (supplemental
329 table S3) and 7500 Fast Real Time PCR System (all Applied Biosystems). To quantify gene

330 expression, the comparative CT method was used as described previously (4, 38, 39) using
331 Glyceraldehyde 3-phosphate dehydrogenase (GAPDH) as internal control.

332

333 **Statistical analysis**

334 Data visualization and statistical analysis were performed using R software version 3.5.1 (R
335 Foundation for Statistical Computing, Vienna, Austria. <https://www.R-project.org>),
336 Microsoft Excel or Graph Pad Prism. Values are expressed as mean +/- standard deviation
337 (SD), or mean +/- 95% confidence interval as indicated in the figures. Statistical significance
338 was analysed using unpaired, non-parametric t-test, or ANOVA. Differences of mRNA
339 expression levels between groups were assessed using Wilcoxon signed-rank test to
340 compare two groups or Kruskal-Wallis test for post hoc analysis to compare more than two
341 groups. Spearman's rank-order correlation was used to test the association between
342 continuous variables. P-value < 0.05 was considered as significant.

343

344 **Results**

345

346 **HCC conditioned medium induces an activated phenotype and activation of the AMPK** 347 **pathway in hHSC.**

348 To investigate the interaction between primary hHSC and HCC cells, we incubated three
349 different hHSC preparations (i.e. cells obtained from three different donors) for 24 hours
350 with conditioned medium obtained from the hepatoblastoma cell line HepG2 (*TP53* gene
351 wild type cells with *CTNNB1* exon3 deletion activating β -catenin), and the HCC cell line
352 PLC/PRF/5 (*TP53* mutation bearing cells with high levels of β -catenin protein expression) (7).
353 Both HCC cell lines belong to transcriptomic class 1 classification including the most
354 differentiated liver cancer cell lines with epithelial features (11). As shown in Figure 1A,
355 conditioned medium of PLC/PRF/5 and HepG2 cells induced a significant increase in
356 expression of several genes associated with hHSC activation, including the collagen
357 crosslinking enzyme lysyl oxidase (LOX) as well as the inflammatory genes IL-1 β , IL-8 and
358 CCL2 in a cancer cell type specific manner. In contrast, 24 hours treatment with HCC cell
359 conditioned medium had no effect on TIMP1 and MMP2 expression, and resulted in
360 downregulation of collagen 1A1 and IL-6 gene expression (Figure 1A). Moreover, hHSC
361 proliferation was significantly increased following incubation with HepG2 conditioned

362 medium compared to serum free medium (Figure 1B), whereas hHSC proliferation remained
363 unchanged when treated with conditioned medium of PLC/PRF/5 cells. As HepG2 cells are
364 hepatoblastoma cells, further differences in the potential of HCC cells to induce hHSC
365 proliferation were confirmed employing conditioned medium of additional HCC cell lines.
366 Thus, HCC cell lines characterized by, amongst numerous other mutations (7, 19, 47),
367 various mutations in cell-cycle regulating genes, such as p53 (PLC/PRF/5, Huh-7, Mahlavu)
368 and β -catenin (HepG2, Huh-6, SNU398) were investigated. Similar to HepG2 cells,
369 conditioned medium of Huh-6 and Huh-7 cells induced hHSC proliferation *in vitro* (Figure
370 1C). In contrast, hHSC proliferation was unchanged following incubation with conditioned
371 medium of SNU398 or Mahlavu cells (Figure 1C), indicating that diverse HCC cell lines
372 differentially affect hHSC proliferation. Overall, these data further confirm that the
373 dysregulation of the cancer cell secretome plays a key role, not only in tumor
374 transformation/progression, but also affects the stromal cells in a HCC cell line specific
375 manner (6, 33, 62). It has been shown previously that cell proliferation is regulated via
376 AMPK and that activation of AMPK in HSC leads to inhibition of PDGF-BB-induced
377 proliferation (9, 41). AMPK activation is characterized by phosphorylation of AMPK at
378 threonine residue 172 of its catalytic subunit α (AMPK-Thr¹⁷²) whereas phosphorylation of
379 AMPK-Ser^{485/491} results in inhibition of AMPK activity (21, 24) (Figure 1E). To test whether
380 activation of the AMPK pathway is associated with the induction of hHSC proliferation by
381 HCC cells, activation of AMPK and its upstream kinase LKB1 were analysed in hHSC after 24
382 hours incubation with HCC cell line conditioned medium. PLC/PRF/5 cell conditioned
383 medium induced a strong phosphorylation of AMPK at Thr¹⁷² and only mild phosphorylation
384 at AMPK-Ser^{485/491} when compared to treatment with serum free medium (SFM), indicating
385 overall activation of AMPK (Figure 1D, Supplemental Figure S1A). In contrast, conditioned
386 medium of HepG2 cells induced a mild phosphorylation of AMPK-Thr¹⁷² associated with a
387 strong phosphorylation of AMPK-Ser^{485/491}, suggesting an overall inhibition of AMPK activity
388 (Figure 1D, Supplemental Figure S1A). Phosphorylation of the AMPK upstream kinase LKB1
389 that regulates phosphorylation of AMPK-Thr¹⁷² was strongly reduced after treatment with
390 the conditioned media of both HCC cell lines, compared to serum free medium (Figure 1D,
391 Supplemental Figure S1A), suggesting that phosphorylation of AMPK-Thr¹⁷² is regulated
392 differently in hHSC treated with conditioned media. Similar to conditioned medium of
393 PLC/PRF/5 cells, conditioned medium of the cancer cell lines SNU398 and Mahlavu induced

394 AMPK activation in hHSC, as suggested by the strong phosphorylation of AMPK-Thr¹⁷², while
395 phosphorylation of AMPK-Thr¹⁷² was only mildly induced or absent following incubation
396 with Huh-6 and Huh-7 conditioned medium (Supplemental Figure S1B). Overall, these
397 results demonstrate the ability of HCC cells to induce hHSC activation, as well as activation
398 of the AMPK pathway in hHSC, with HCC cell line specific features.

399

400 **AICAR and Compound C inhibit hHSC activation induced by HCC cells**

401 We next investigated the effect of the pharmacological agents AICAR (15, 54) and
402 Compound C (1), known to affect AMPK signalling. We first assessed the effect of both
403 pharmacological agents on AMPK activation/phosphorylation in hHSC, as well as their effect
404 on metabolic activity, proliferation and hHSC gene expression. We observed an increase in
405 AMPK phosphorylation at Thr¹⁷² in hHSC treated with AICAR whereas p-AMPK-Thr¹⁷² was
406 absent in hHSC exposed to Compound C (Figure 2A). Further, we did not observe changes in
407 phosphorylation of AMPK-Ser^{485/491} following treatment with AICAR or Compound C
408 compared to the untreated control (Figure 2A), suggesting activation of AMPK through
409 AICAR but not Compound C. The metabolic activity and proliferation in hHSC were
410 significantly inhibited by both pharmacological agents in a dose-dependent manner
411 indicating that both AICAR and Compound C can inhibit hHSC activation (Figure 2B – 2C)
412 without inducing cell death as assessed by cell death ELISA (Figure 2D).

413 We next investigated the effect of both pharmacological agents on HCC-induced hHSC
414 activation by treating hHSC with conditioned medium of HepG2 or PLC/PRF/5 cells and
415 AICAR or Compound C in parallel. As demonstrated in Figure 2E, treatment with AICAR was
416 sufficient to abrogate the induction of inflammatory gene expression by HepG2 and
417 PLC/PRF/5 conditioned medium in hHSC, while expression of LOX was unchanged. This
418 effect was less prominent in hHSC exposed to Compound C (Supplemental Figure S2A).
419 Moreover, both AICAR and Compound C were able to reverse HepG2 induced proliferation
420 in hHSC (Figure 2F). Similarly, proliferation of HepG2 and PLC/PRF/5 cells treated with
421 conditioned medium of hHSC was inhibited following treatment with AICAR and Compound
422 C (Supplemental Figure S2B and S2C). These data indicate that both AICAR and Compound C
423 inhibit the cross-talk between HCC and hHSC and *vice versa*. Next, protein expression
424 analysis was performed and showed that AICAR could induce p-AMPK-Thr¹⁷² expression in
425 hHSC treated with conditioned medium of PLC/PRF/5 and HepG2 cells. These effects were

426 not observed when hHSC were exposed to Compound C in combination with HCC
427 conditioned medium (Figure 2F), indicating that the inhibitory effect of Compound C might
428 be AMPK-independent. Taken together, these data show that both AICAR and Compound C
429 are potent inhibitors of hHSC activation and are able to reverse HCC-induced hHSC
430 proliferation and activation *in vitro*.

431

432 **AICAR and Compound C inhibit MEF proliferation in an AMPK independent manner**

433 Although AMPK is known as a crucial regulator of cell proliferation, pharmacological AMPK
434 modulating agents have been shown to act both in an AMPK-dependent and -independent
435 manner (34, 35, 46, 59, 60). Likewise, the previous set of data suggested that inhibition of
436 hHSC proliferation and metabolic activity by AICAR and Compound C (Figure 2) may be
437 driven by both AMPK-dependent and AMPK-independent signals. To further test this
438 hypothesis, we employed mouse embryonic fibroblasts (MEFs) deficient of both existing
439 isoforms of the catalytic AMPK isoform α (AMPK ^{$\alpha 1/\alpha 2$ -/-} i.e. DKO) and wild type (wt) MEFs
440 (30). Cells were treated with AICAR or Compound C for 24 hours and a significant, dose-
441 dependent reduction of metabolic activity was observed in wt MEFs as well as in AMPK ^{$\alpha 1/\alpha 2$ -}
442 ^{-/-} MEFs (Figure 3A, 3B). Moreover, AICAR and Compound C showed a trend to inhibit cell
443 proliferation in wt MEFs and AMPK ^{$\alpha 1/\alpha 2$ -/-} MEFs (Figure 3C, 3D).

444

445 **AICAR and Compound C regulate hHSC cell proliferation through AMPK-dependent and** 446 **AMPK-independent mechanisms**

447 We next aimed at unravelling the pathways and mechanisms through which AICAR and
448 Compound C inhibited proliferation of hHSC and MEFs and their dependency on AMPK.
449 First, cell cycle analysis was performed on hHSC treated with 1mM AICAR or 10 μ M
450 Compound C for 24 hours. As shown in Figure 4A, both AICAR and Compound C induced cell
451 cycle arrest in hHSC in the S-phase. When analysing the cell cycle in MEFs treated with
452 AICAR or Compound C, we surprisingly observed inhibition of the cell cycle in both wt and
453 AMPK ^{$\alpha 1/\alpha 2$ -/-} MEFs, with AICAR inhibiting the cell cycle in the S-phase and Compound C in the
454 G1-phase, respectively (Figure 4B). These data suggest that both Compound C and AICAR
455 can induce cell cycle arrest independently of AMPK.

456 Next, the mammalian target of rapamycin (mTOR), a critical regulator of cell metabolism
457 and proliferation, was investigated to test another signalling pathway by which AICAR and
458 Compound C may inhibit cell proliferation. Although mTOR is downstream of AMPK (20), the
459 pathway can alternatively be regulated through various other pathways (51). The mTOR
460 complex 1 (mTORC1) mediates its effects through phosphorylation of its downstream
461 targets eukaryotic initiation factor 4E (eIF4E)-binding protein 1 (4E-BP1) and the p70
462 ribosomal S6 kinase (S6) (31). Thus, hHSC were treated with 1mM AICAR or 10 μ M
463 Compound C for 24 hours and phosphorylation of S6 and 4E-BP1 proteins was assessed.
464 Figure 4C demonstrates that phosphorylation of 4E-BP1 was mildly reduced, whereas
465 phosphorylation of S6 was abrogated following treatment with AICAR, but not upon
466 Compound C exposure (Supplemental Figure S3A). These data show that AICAR, but not
467 Compound C, inhibits cell proliferation through mTORC1 inhibition in hHSC. To further test
468 whether AICAR inhibited mTORC1 in an AMPK-dependent manner, wt MEFs and AMPK ^{α 1/ α 2-}
469 ^{-/-} MEFs were treated with AICAR for 24 hours. As shown in Figure 4D, phosphorylation of 4E-
470 BP1 was slightly reduced and phosphorylation of S6 was abrogated in AICAR treated wt
471 MEFs. In contrast, such reduction of 4E-BP1 and S6 phosphorylation did not occur in
472 AMPK ^{α 1/ α 2-} MEFs (Figure 4D, Supplemental Figure S3A), indicating that AICAR inhibits
473 mTORC1 in wt MEFs, as well as in hHSC, in an AMPK-dependent manner. The data further
474 show that Compound C only mildly reduced phosphorylation of 4E-BP1 in wt MEFs, and that
475 S6 phosphorylation was unchanged in wt MEFs and AMPK ^{α 1/ α 2-} MEFs, clearly indicating that
476 Compound C does not affect the mTORC1 pathway in MEFs or hHSC (Figure 4D). Overall,
477 these data show that both AICAR and Compound C inhibit cell proliferation through
478 different pathways involving both AMPK-dependent and independent mechanisms.

479

480 **AMPK gene expression is overexpressed in a subset of HCC patients.**

481 In order to further investigate possible changes in AMPK gene expression during the process
482 of HCC we analysed the gene expression level of both isoforms of the catalytic AMPK α
483 isoforms i.e. AMPK α 1 (*PRKAA1*) and AMPK α 2 (*PRKAA2*) in 2 independent cohorts of HCC
484 tissue i.e. the TCGA and LICA-FR (3). In both cohorts, samples were excluded when carrying
485 both the *TP53* and *CTNNB1* gene mutations. The main difference between both cohorts
486 concerns aetiology, i.e. the TCGA cohort is enriched by HBV patients and contains a lower

487 amount of patients featuring the CTNNB1 mutation rate. In contrast, there is no significant
488 difference in the METAVIR fibrosis score between the two cohorts (Supplemental Table S1).
489 A correlation analysis was performed and showed that *PRKAA1* and *PRKAA2* expression
490 levels are not associated (Figure 5A, LICA-FR: $R = -0.101$, P value=ns and TCGA: $R = -0.026$, P
491 value=ns). Next, *PRKAA1* and *PRKAA2* expression was analysed and no significant correlation
492 was found in tumours carrying the *TP53* mutation (Supplemental Figure S4). In contrast, a
493 significant association was demonstrated between *PRKAA1* and *CTNNB1* mutation in the
494 TCGA dataset but not in LICA-FR, whereas a significant association was demonstrated
495 between *PRKAA2* expression and tumours carrying the *CTNNB1* gene mutation in both
496 cohorts (Figure 5B). Importantly, a positive correlation was observed between *PRKAA2*
497 expression and *CTNNB1* target genes such as Glutamate-Ammonia Ligase (GLUL), Leucine
498 Rich Repeat Containing G Protein-Coupled Receptor 5 (LGR5) and Laminin Subunit Alpha 3
499 (LAMA3) in both datasets confirming that *PRKAA2* is a potential *CTNNB1* target gene (Figure
500 5C).

501 Furthermore, both *PRKAA1* and *PRKAA2* expression were compared in both datasets by
502 using Edmondson grading (I-II and III-IV) and the previous described unsupervised
503 transcriptome analysis (5) which classifies human HCC tumours in 6 subgroups (G1 to G6).
504 *PRKAA1* gene expression showed no significant correlation with different degrees in
505 Edmondson grading (I-II and III-IV) (Supplemental Figure S5A and S5E) and G1 *versus* G6
506 subgroups (Supplemental Figure S5B and S5F) in both datasets. In contrast, *PRKAA2*
507 expression showed significant differences between grade I-II *versus* III-IV ($P = 0.011$, LICA-FR
508 dataset, Supplemental Figure S5C), whereas no significant correlation was found in the
509 TCGA dataset. Notably, in both datasets a high *PRKAA2* expression was found in G5-G6
510 subgroups in line with its association with *CTNNB1* gene mutations (Supplemental Figure
511 S5D and S5H).

512 Furthermore, IHC for the detection of AMPK α 1 was performed on formalin fixed paraffin-
513 embedded human liver sections from histologically normal liver, cirrhotic liver without HCC
514 and HCC in the context of a cirrhotic liver (Supplemental Figure S6). AMPK α 1 weakly stained
515 the hepatocyte membranes in both normal liver tissue and cirrhotic liver tissue without HCC
516 (Supplemental Figure S6A and S6B). Similar localization was observed in cirrhotic tissue
517 surrounding the HCC lesion. AMPK α 1 staining showed a stronger membrane staining with
518 some cytoplasm staining in the HCC tumour tissue of patient with grade 1 (Supplemental

519 Figure S6C). Further, the tumour tissue of grade 2 classified patient showed a strong
520 cytoplasmic staining for AMPK α 1, which appeared even stronger in the HCC tissue classified
521 as grade 3 (Supplemental Figure S6D and S6E).

522 Overall, these data, although reflecting the heterogeneity in human HCC (37), suggest an
523 important role for AMPK modulation for the development of novel therapeutic strategies
524 against HCC.

525

526

527

528 **Discussion**

529 HCC is one of the leading causes for cancer death worldwide (18, 27). In spite of the recent
530 progress in treatment options for HCC with the introduction of new multi-kinase inhibitors
531 and immune-therapy (36), the identification of new therapeutic targets, more widely
532 reflecting HCC biology, represents a current crucial effort in Oncology.

533 The tumour microenvironment plays a crucial role in HCC development and progression (10,
534 37), as over 80% of HCC develop on the background of liver fibrosis and cirrhosis (56). In this
535 context, genetic alterations and deregulation of signalling pathways are the result of chronic
536 hepatocellular necrosis, inflammation, oxidative stress and a dysregulated extracellular
537 matrix (ECM) deposition which further favours cancer development (10, 22). Moreover, in a
538 previous study we identified, by proteomic analysis, specific enriched proteins in the human
539 cirrhotic ECM in comparison to healthy ECM proteins. Culturing the cells in a stiffer cirrhotic
540 3D microenvironment demonstrated the unique up-regulation in genes related to epithelial
541 to mesenchymal transition (EMT) and TGF β signalling. Further demonstrating that the
542 inherent features of the human cirrhotic liver ECM are key pro-carcinogenic components in
543 HCC (40). One of the key hallmarks of the development of liver fibrosis is the activation of
544 HSC (42). Recent evidence showed that the bi-directional cross-talk between activated HSC
545 and HCC cells promotes HCC cell proliferation and tumour growth (2, 16), in addition to
546 favouring a pro-inflammatory and pro-fibrogenic microenvironment (16). Here, we
547 investigated the potential paracrine effect of different HCC cell lines to activate primary
548 human HSC and the possible implication of AMPK in the HCC-induced activation of hHSC. As
549 HCC is known to be a highly heterogeneous cancer (8, 17) several HCC cell lines were

550 investigated in this study. These cell lines are characterized by different mutations in cell-
551 cycle regulating genes such as p53 (PLC/PRF/5, Huh-7, Mahlavu) and β -catenin (HepG2,
552 Huh-6, SNU398) (7, 19, 47) and express a characteristic secretome (6, 33, 62). Besides
553 exerting different effects on hHSC proliferation and gene expression, HCC conditioned
554 media differentially activated the AMPK pathway in hHSC, again emphasizing the complexity
555 of HCC heterogeneity by possibly affecting the stromal compartment through AMPK
556 induction. Indeed, when datamining 2 independent cohorts of HCC tissues i.e. the TCGA and
557 LICA-FR we showed no significant correlation between tumours carrying the *TP53* mutation
558 and both catalytic AMPK α isoforms, whereas a significant correlation was found between
559 tumours carrying the *CTNNB1* gene mutation and the AMPK α isoforms. It is known that
560 *CTNNB1* and *TP53* mutations are affecting 25-30% of HCC patients and both mutations are
561 defined by different subgroups in HCC and correlate with better or worse patient outcome,
562 respectively (5, 8, 11). Another layer of complexity may emerge knowing that in certain
563 cancer cell lines and primary tumours a correlation has been demonstrated between
564 *PRKAA1* gene copy number and mRNA expression suggesting that gene amplification does
565 lead to increased expression, whereas the frequency of alterations in the *PRKAA2* gene in
566 cancer is lower overall (12, 29). Moreover, recent studies have shown that the liver
567 microenvironment may play a crucial role in NAFLD/NASH towards HCC progression. Such
568 changes in HCC incidence are affected by obesity, type 2 diabetes, and NAFLD, which is the
569 most common liver disease and marked by aberrant AMPK activity (43, 65). Indeed, in a
570 previous study an unbiased transcriptomic and ingenuity pathway analysis revealed no
571 AMPK-related pathway enrichment in NAFLD patients. Nevertheless, a list of AMPK related
572 genes, unbiasedly generated by means of STRING analysis and UCSC Genome Browser data
573 mining tool goldenPath, showed to be significantly affected in the RNA sequence data of
574 patients with NAFLD *versus* healthy controls. Several AMPK subunits such as *PRKAB1*,
575 *PRKAB2*, *PRKAG1* were significantly downregulated in NAFLD patients. Most strikingly, a
576 perturbation was found in many AMPK pathway genes such as *TBC1D1*, *SLC2A4/GLUT4*,
577 *AKT1/2*, and genes involved in the regulation of lipid metabolism and
578 activation/phosphorylation of AMPK such as *Sirt3* and *TSC2* in NAFLD patients (64).
579 AMPK α 1 is widely expressed across tissues, whereas AMPK α 2 is more restricted in its tissue-
580 and intracellular distribution (29, 50). Both AMPK α isoforms are expressed in human healthy
581 and diseased liver tissue (12, 44, 64). Furthermore, we demonstrated that primary hHSC

582 express more isoform AMPK α 1 than AMPK α 2 (39). Besides changes of AMPK α 1/ α 2 gene
583 expression in HCC, posttranslational modifications, such as the phosphorylation of AMPK
584 are important in the development/progression of HCC as was demonstrate by Jiang et al,
585 that the risk of HCC occurrence was significantly higher in patients with a low expression of
586 p-AMPK (28). In this study, we demonstrate that HCC-induced activation of hHSC can involve
587 AMPK and its phosphorylation. Importantly, the catalytic AMPK subunit α can be
588 phosphorylated at different phosphorylation sites (61). While phosphorylation at Thr¹⁷²
589 activates AMPK (55), phosphorylation at Ser^{485/491} inhibits its activity and favours
590 dephosphorylation at Thr-172 (24, 26). We demonstrate that, depending on the HCC cell
591 line used, either phosphorylation of AMPK-Ser^{485/491} or phosphorylation of AMPK-Thr¹⁷² can
592 be achieved by HCC cells. This further resulted in differences observed in hHSC proliferation.
593 In this study, we also provide new evidence for the possible working mechanisms of
594 pharmacological agents known as AMPK activators and inhibitors in the cross-talk between
595 hHSC and HCC. Here, we demonstrate that the AMPK activator AICAR inhibits both the
596 proliferation and the pro-fibrogenic and pro-inflammatory phenotype of primary human
597 HSC in a dose-dependent manner under basal conditions as well as after exposure to HCC
598 conditioned medium. Indeed, pharmacologically induced AMPK activation has been shown
599 to exert anti-HCC properties by inhibiting proliferation through AICAR (14, 32) and the
600 incidence of several tumour types, including HCC, has been shown to be lower in patients
601 treated with the AMPK activator and oral anti-diabetic drug metformin (13). Our data
602 reinforce the concept that AMPK activation may be beneficial for tumour-stromal
603 interactions in HCC, as it can target both hHSC and HCC cells. Therefore, our data add new
604 evidence about pharmacological AMPK activators and their effect on HCC-induced
605 proliferation in primary hHSC.

606 Next, we demonstrate in more detail an AMPK-dependent but also AMPK-independent
607 working mechanisms of Compound C, a known AMPK inhibitor, which inhibits proliferation
608 and induces cancer cell death (25, 34, 63). Treatment with Compound C showed significant,
609 dose-dependent anti-proliferative effects on hHSC to the same extent as the AMPK activator
610 AICAR without affecting the inhibitory phosphorylation of AMPK-Ser^{485/491}, suggesting
611 AMPK-independent effects. Indeed, recent evidence suggests that Compound C exerts
612 AMPK-independent anti-proliferative effects in different cancers, by inducing apoptosis,
613 inhibiting Akt and the mTOR signalling pathway, as well as induction of cell cycle arrest (1,

614 34). Unlike in cancer cells (34, 63), Compound C did not induce apoptosis in primary human
615 HSC and did not modulate mTOR signalling pathway. However, we show that Compound C
616 induces cell cycle arrest in the S-phase in hHSC, as well as in the G1-phase in MEFs and
617 independently of AMPK. Moreover, we show that treatment with AICAR inhibits the
618 mTORC1 pathway in primary hHSC, as well as in wt MEFs in an AMPK-dependent manner.
619 Overall, our data show that AICAR and Compound C inhibit hHSC proliferation through
620 different mechanisms, some of which are AMPK-dependent.

621 This study clearly demonstrates the existence of a cross-talk between human HCC cells and
622 primary human HSC which affects hHSC activation, as well as activation of the AMPK
623 pathway in hHSC, pointing towards a role for AMPK in tumour stromal interactions in HCC
624 development. Moreover, the data show that pharmacological AMPK activation of the anti-
625 proliferative pharmacological compounds AICAR and Compound C could represent a novel
626 approach for anti-cancer and anti-fibrotic therapy.

627

628

629 **Figure legends**

630

631 **Figure 1. HCC conditioned medium activates hHSC and affects the AMPK pathway in hHSC.**

632 (A) Gene expression and (B) proliferation response in hHSC following treatment with
 633 conditioned medium of HepG2 or PLC/PRF/5 cells for 24h. (C) Proliferation of hHSC
 634 following 24h treatment with different HCC conditioned media. (D) AMPK phosphorylation
 635 profile expression in hHSC after exposure with HepG2 or PLC/PRF/5 conditioned medium for
 636 24h. (E) Schematic of AMPK phosphorylation sites and AMPK activation/inhibition. (A) Data
 637 represent mean +/- 95% confidence interval, *p = 0.05, pooled data of 3 independent
 638 experiments, (B-D) Representative data of at least 3 independent experiments, data
 639 represent mean +/- SD, **** p<0.0001, ns = not significant vs. SFM. CM = complete
 640 medium, SFM = serum free medium.

641

642 **Figure 2: AICAR and Compound C reverse HCC-induced hHSC activation.**

643 (A) AMPK phosphorylation profile in hHSC treated with AICAR and Compound C. Human HSC
 644 metabolic activity and proliferation following 24h treatment with (B) AICAR (0.25-4mM) or
 645 (C) Compound C (2.5-40μM). (D) Quantification of nucleosome expression by ELISA in hHSC
 646 following 24h treatment with AICAR or Compound C. (E) Gene expression, (F) proliferation
 647 and protein expression in hHSC following 24h treatment with PLC/PRF/5 or HepG2
 648 conditioned medium and AICAR (1mM) or Compound C (10μM). (B)-(D), (F) Data represent
 649 mean +/- SD, *p< 0.05, **p<0.01, ***p<0.001, ****p<0.0001 vs. SFM and #p< 0.05 vs. non-
 650 AICAR treated control. (e) Data represent mean +/- 95% confidence interval, *p = 0.05 vs.
 651 serum free medium, #p = 0.05 vs. non-AICAR treated control. (A) – (F) Representative data of
 652 at least 3 independent experiments. CM = complete medium, SFM = serum free medium,
 653 c.m. = conditioned medium, CC = Compound C.

654

655 **Figure 3: AICAR and Compound C inhibit hHSC metabolic activity and proliferation**
 656 **independently of AMPK.**

657 (A-B) Metabolic activity and (C-D) proliferation in wt and AMPK^{α1/α2-/-} (DKO) MEFs following
 658 24h treatment with AICAR and Compound C. (A) – (D) Data represent mean +/- SD
 659 ***p<0.001, ****p<0.0001 vs. SFM (wt), ##p<0.01, ###p<0.001, ####p<0.0001 vs. SFM

660 (AMPK ^{α 1/ α 2^{-/-}}), ⁺p<0.05, ⁺⁺⁺⁺p<0.0001 as indicated, representative data of at least 3
661 independent experiments. SFM = serum free medium, DKO = AMPK ^{α 1/ α 2^{-/-}}
662

663 **Figure 4: AICAR and Compound C inhibit hHSC proliferation through various mechanisms.**

664 (A) Cell cycle analysis in hHSC following treatment with 1mM AICAR or 10 μ M Compound C
665 for 24h. (B) Cell cycle analysis in wt and AMPK α 1/ α 2^{-/-} MEFs following treatment with
666 0.5mM AICAR and 10 μ M Compound C for 24h. (C) Protein expression in hHSC following
667 treatment with 1mM AICAR or 10 μ M Compound C for 24h. (D) Protein expression in wt and
668 AMPK α 1/ α 2^{-/-} MEFs following 24h treatment with 0.25mM AICAR and 10 μ M Compound C.
669 (A) – (D) Representative data of at least 3 independent experiments. SFM = serum free
670 medium, CC = Compound C, CM = complete medium.

671

672 **Figure 5: Validation of AMPK gene expression in a subset of HCC patients.**

673 Gene expression levels of AMPK α 1 (*PRKAA1*) and AMPK α 2 (*PRKAA2*) were investigated in 2
674 independent cohorts of HCC (TCGA and LICA-FR). (A) Correlation analysis showed that
675 *PRKAA1* and *PRKAA2* expression levels are not associated (Spearman's R=-0.101 LICA-FR, P
676 value=ns and Spearman's R=-0.026, P value=ns in TCGA). (B) A significant association was
677 observed between *PRKAA1* and *CTNNB1* gene mutations in the TCGA cohort but not in the
678 LICA-FR dataset. A significant association was demonstrated between *PRKAA2* expression
679 and tumours carrying the *CTNNB1* gene mutation in both cohorts (Wilcoxon signed-rank
680 test). (C) A positive correlation was observed between *PRKAA2* expression and *CTNNB1*
681 target genes such as *GLUL*, *LGR5* and *LAMA3* in both datasets confirming that *PRKAA2* is a
682 potential *CTNNB1* target gene (Spearman's rank-order correlation, p value <0.0001
683 (M=mutant, NM= non-mutant).

684

685

686 **Bibliography**

687

688

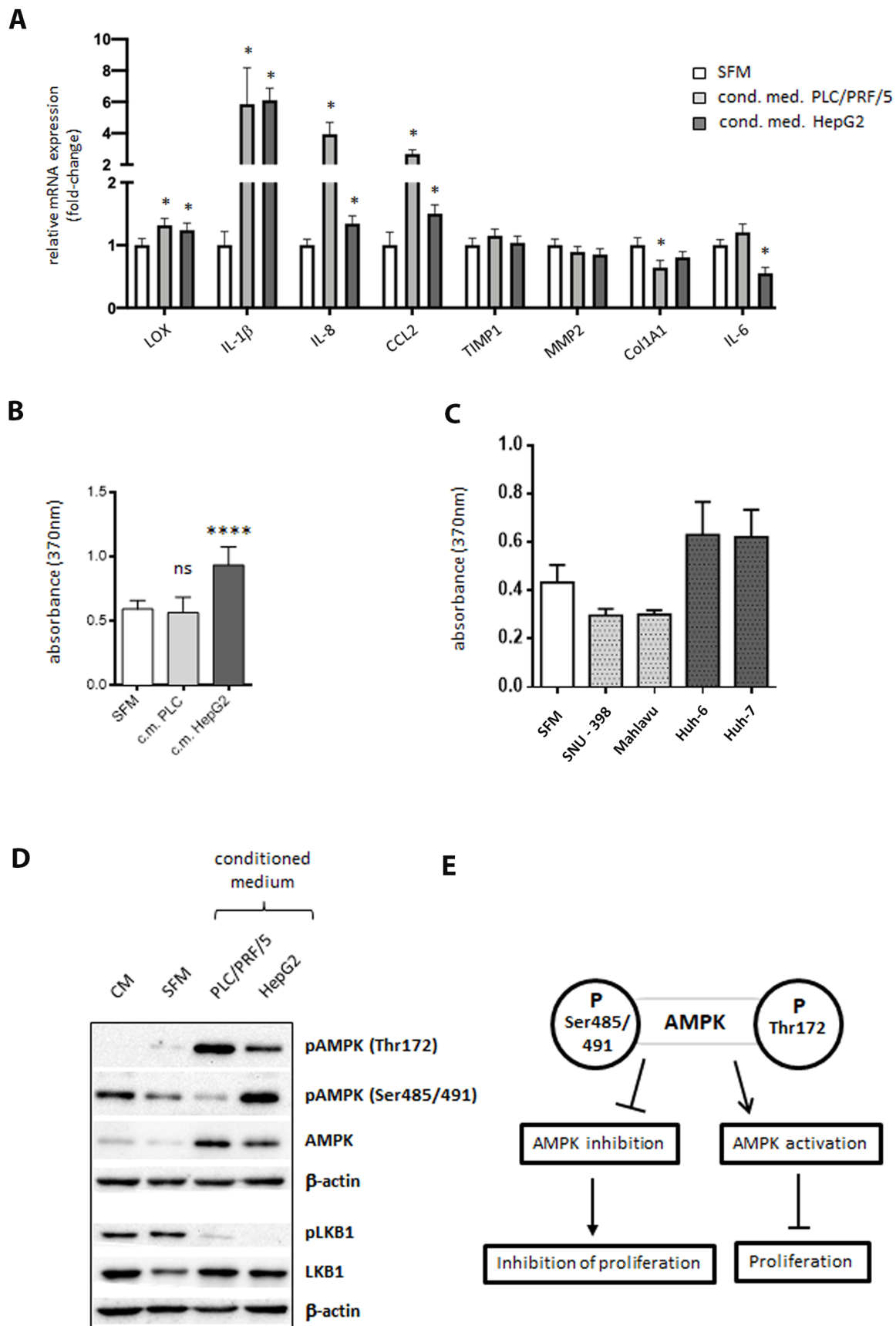
- 689 1. **Adachi M, and Brenner DA.** High molecular weight adiponectin inhibits proliferation
690 of hepatic stellate cells via activation of adenosine monophosphate-activated protein
691 kinase. *Hepatology* 47: 677-685, 2008.
- 692 2. **Amann T, Bataille F, Spruss T, Muhlbauer M, Gabele E, Scholmerich J, Kiefer P,**
693 **Bosserhoff AK, and Hellerbrand C.** Activated hepatic stellate cells promote tumorigenicity of
694 hepatocellular carcinoma. *Cancer Sci* 100: 646-653, 2009.
- 695 3. **Bayard Q, Meunier L, Peneau C, Renault V, Shinde J, Nault JC, Mami I, Couchy G,**
696 **Amaddeo G, Tubacher E, Bacq D, Meyer V, La Bella T, Debaillon-Vesque A, Bioulac-Sage P,**
697 **Seror O, Blanc JF, Calderaro J, Deleuze JF, Imbeaud S, Zucman-Rossi J, and Letouze E.** Cyclin
698 A2/E1 activation defines a hepatocellular carcinoma subclass with a rearrangement
699 signature of replication stress. *Nature communications* 9: 5235, 2018.
- 700 4. **Bottcher K, Rombouts K, Saffioti F, Roccarina D, Rosselli M, Hall A, Luong T,**
701 **Tsochatzis EA, Thorburn D, and Pinzani M.** MAIT cells are chronically activated in patients
702 with autoimmune liver disease and promote pro-fibrogenic hepatic stellate cell activation.
703 *Hepatology* 2018.
- 704 5. **Boyault S, Rickman DS, de RA, Balabaud C, Rebouissou S, Jeannot E, Herault A,**
705 **Saric J, Belghiti J, Franco D, Bioulac-Sage P, Laurent-Puig P, and Zucman-Rossi J.**
706 Transcriptome classification of HCC is related to gene alterations and to new therapeutic
707 targets. *Hepatology* 45: 42-52, 2007.
- 708 6. **Brown KJ, Formolo CA, Seol H, Marathi RL, Duguez S, An E, Pillai D, Nazarian J,**
709 **Rood BR, and Hathout Y.** Advances in the proteomic investigation of the cell secretome.
710 *Expert Rev Proteomics* 9: 337-345, 2012.
- 711 7. **Cagatay T, and Ozturk M.** P53 mutation as a source of aberrant beta-catenin
712 accumulation in cancer cells. *Oncogene* 21: 7971-7980, 2002.
- 713 8. **Calderaro J, Ziol M, Paradis V, and Zucman-Rossi J.** Molecular and histological
714 correlations in liver cancer. *Journal of hepatology* 2019.
- 715 9. **Caligiuri A, Bertolani C, Guerra CT, Aleffi S, Galastri S, Trappoliere M, Vizzutti F,**
716 **Gelmini S, Laffi G, Pinzani M, and Marra F.** Adenosine monophosphate-activated protein
717 kinase modulates the activated phenotype of hepatic stellate cells. *Hepatology* 47: 668-676,
718 2008.
- 719 10. **Carloni V, Luong TV, and Rombouts K.** Hepatic stellate cells and extracellular matrix
720 in hepatocellular carcinoma: more complicated than ever. *Liver Int* 2014.
- 721 11. **Caruso S, Calatayud AL, Pilet J, La Bella T, Rekik S, Imbeaud S, Letouze E, Meunier L,**
722 **Bayard Q, Rohr-Udilova N, Peneau C, Grasl-Kraupp B, de Koning L, Ouine B, Bioulac-Sage P,**
723 **Couchy G, Calderaro J, Nault JC, Zucman-Rossi J, and Rebouissou S.** Analysis of Liver Cancer
724 Cell Lines Identifies Agents With Likely Efficacy Against Hepatocellular Carcinoma and
725 Markers of Response. *Gastroenterology* 2019.
- 726 12. **Cerami E, Gao J, Dogrusoz U, Gross BE, Sumer SO, Aksoy BA, Jacobsen A, Byrne CJ,**
727 **Heuer ML, Larsson E, Antipin Y, Reva B, Goldberg AP, Sander C, and Schultz N.** The cBio
728 cancer genomics portal: an open platform for exploring multidimensional cancer genomics
729 data. *Cancer Discov* 2: 401-404, 2012.

- 730 13. **Chen HP, Shieh JJ, Chang CC, Chen TT, Lin JT, Wu MS, Lin JH, and Wu CY.** Metformin
731 decreases hepatocellular carcinoma risk in a dose-dependent manner: population-based
732 and in vitro studies. *Gut* 62: 606-615, 2013.
- 733 14. **Cheng J, Huang T, Li Y, Guo Y, Zhu Y, Wang Q, Tan X, Chen W, Zhang Y, Cheng W,**
734 **Yamamoto T, Jing X, and Huang J.** AMP-activated protein kinase suppresses the in vitro and
735 in vivo proliferation of hepatocellular carcinoma. *PloS one* 9: e93256, 2014.
- 736 15. **Corton JM, Gillespie JG, Hawley SA, and Hardie DG.** 5-aminoimidazole-4-
737 carboxamide ribonucleoside. A specific method for activating AMP-activated protein kinase
738 in intact cells? *European journal of biochemistry / FEBS* 229: 558-565, 1995.
- 739 16. **Coulouarn C, Corlu A, Glaize D, Guenon I, Thorgeirsson SS, and Clement B.**
740 Hepatocyte-stellate cell cross-talk in the liver engenders a permissive inflammatory
741 microenvironment that drives progression in hepatocellular carcinoma. *Cancer Res* 72:
742 2533-2542, 2012.
- 743 17. **Dhanasekaran R, Nault JC, Roberts LR, and Zucman-Rossi J.** Genomic Medicine and
744 Implications for Hepatocellular Carcinoma Prevention and Therapy. *Gastroenterology* 156:
745 492-509, 2019.
- 746 18. **Ferlay J, Soerjomataram I, Dikshit R, Eser S, Mathers C, Rebelo M, Parkin DM,**
747 **Forman D, and Bray F.** Cancer incidence and mortality worldwide: sources, methods and
748 major patterns in GLOBOCAN 2012. *Int J Cancer* 136: E359-386, 2015.
- 749 19. **Forbes SA, Bhamra G, Bamford S, Dawson E, Kok C, Clements J, Menzies A, Teague**
750 **JW, Futreal PA, and Stratton MR.** The Catalogue of Somatic Mutations in Cancer (COSMIC).
751 *Curr Protoc Hum Genet* Chapter 10: Unit 10 11, 2008.
- 752 20. **Gwinn DM, Shackelford DB, Egan DF, Mihaylova MM, Mery A, Vasquez DS, Turk BE,**
753 **and Shaw RJ.** AMPK phosphorylation of raptor mediates a metabolic checkpoint. *Mol Cell*
754 30: 214-226, 2008.
- 755 21. **Hawley SA, Davison M, Woods A, Davies SP, Beri RK, Carling D, and Hardie DG.**
756 Characterization of the AMP-activated protein kinase kinase from rat liver and identification
757 of threonine 172 as the major site at which it phosphorylates AMP-activated protein kinase.
758 *The Journal of biological chemistry* 271: 27879-27887, 1996.
- 759 22. **Hernandez-Gea V, Toffanin S, Friedman SL, and Llovet JM.** Role of the
760 Microenvironment in the Pathogenesis and Treatment of Hepatocellular Carcinoma.
761 *Gastroenterology* 2013.
- 762 23. **Hirsch TZ, Negulescu A, Gupta B, Caruso S, Noblet B, Couchy G, Bayard Q, Meunier**
763 **L, Morcrette G, Scoazec JY, Blanc JF, Amaddeo G, Nault JC, Bioulac-Sage P, Ziolkowski M,**
764 **Beaufrere A, Paradis V, Calderaro J, Imbeaud S, and Zucman-Rossi J.** BAP1 mutations
765 define a homogeneous subgroup of hepatocellular carcinoma with fibrolamellar-like
766 features and activated PKA. *Journal of hepatology* 2019.
- 767 24. **Horman S, Vertommen D, Heath R, Neumann D, Mouton V, Woods A, Schlattner U,**
768 **Wallimann T, Carling D, Hue L, and Rider MH.** Insulin antagonizes ischemia-induced Thr172
769 phosphorylation of AMP-activated protein kinase alpha-subunits in heart via hierarchical
770 phosphorylation of Ser485/491. *The Journal of biological chemistry* 281: 5335-5340, 2006.
- 771 25. **Huang SW, Wu CY, Wang YT, Kao JK, Lin CC, Chang CC, Mu SW, Chen YY, Chiu HW,**
772 **Chang CH, Liang SM, Chen YJ, Huang JL, and Shieh JJ.** p53 modulates the AMPK inhibitor
773 compound C induced apoptosis in human skin cancer cells. *Toxicol Appl Pharmacol* 267: 113-
774 124, 2013.
- 775 26. **Hurley RL, Barre LK, Wood SD, Anderson KA, Kemp BE, Means AR, and Witters LA.**
776 Regulation of AMP-activated protein kinase by multisite phosphorylation in response to

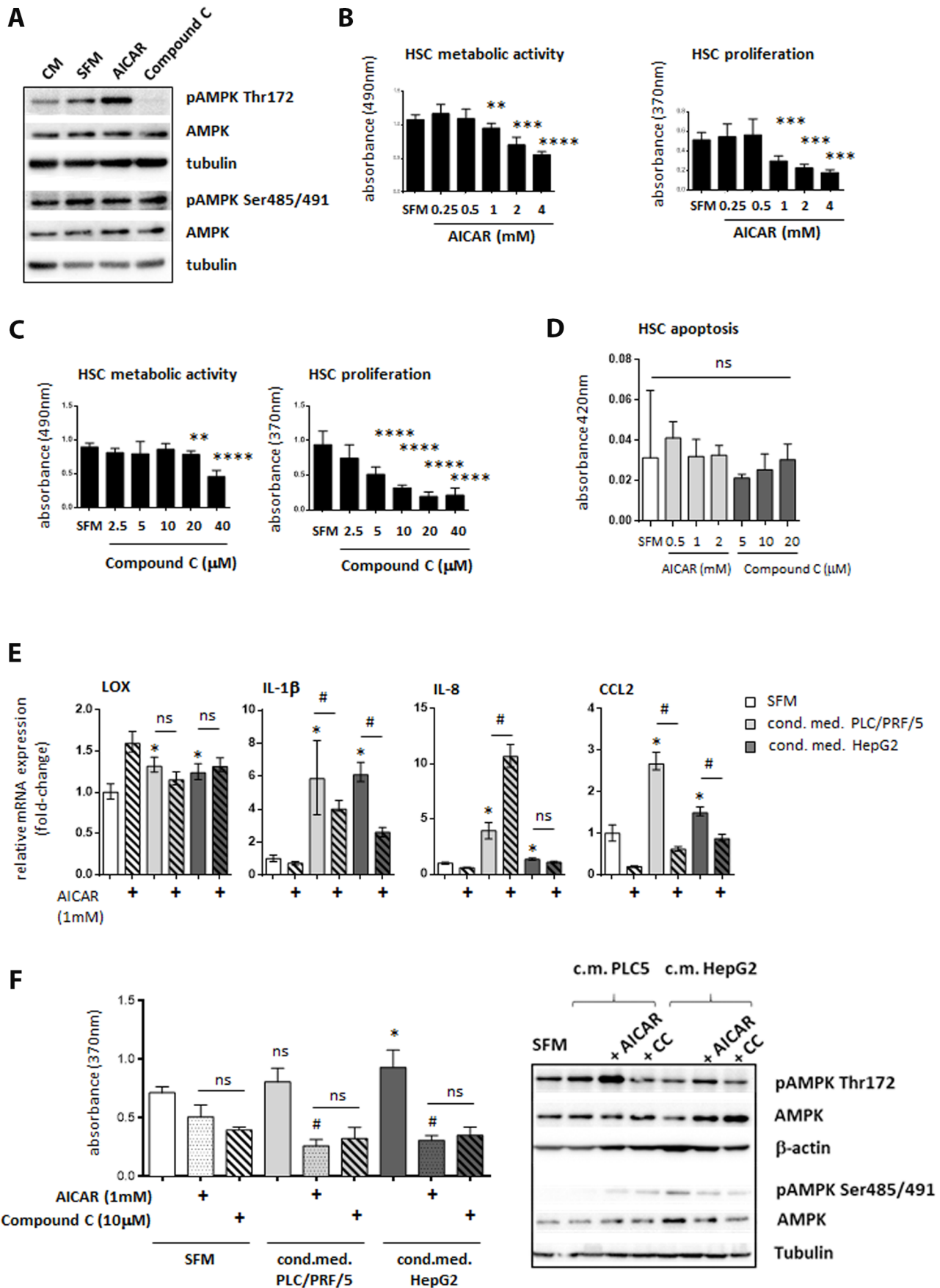
- 777 agents that elevate cellular cAMP. *The Journal of biological chemistry* 281: 36662-36672,
778 2006.
- 779 27. **Jemal A, Bray F, Center MM, Ferlay J, Ward E, and Forman D.** Global cancer
780 statistics. *CA Cancer J Clin* 61: 69-90, 2011.
- 781 28. **Jiang X, Tan HY, Teng S, Chan YT, Wang D, and Wang N.** The Role of AMP-Activated
782 Protein Kinase as a Potential Target of Treatment of Hepatocellular Carcinoma. *Cancers*
783 (*Basel*) 11: 2019.
- 784 29. **Kazgan N, Williams T, Forsberg LJ, and Brenman JE.** Identification of a nuclear
785 export signal in the catalytic subunit of AMP-activated protein kinase. *Mol Biol Cell* 21: 3433-
786 3442, 2010.
- 787 30. **Laderoute KR, Amin K, Calaoagan JM, Knapp M, Le T, Orduna J, Foretz M, and**
788 **Viollet B.** 5'-AMP-activated protein kinase (AMPK) is induced by low-oxygen and glucose
789 deprivation conditions found in solid-tumor microenvironments. *Molecular and cellular*
790 *biology* 26: 5336-5347, 2006.
- 791 31. **Laplante M, and Sabatini DM.** mTOR signaling at a glance. *Journal of cell science*
792 122: 3589-3594, 2009.
- 793 32. **Lee CW, Wong LL, Tse EY, Liu HF, Leong VY, Lee JM, Hardie DG, Ng IO, and Ching YP.**
794 AMPK promotes p53 acetylation via phosphorylation and inactivation of SIRT1 in liver cancer
795 cells. *Cancer Res* 72: 4394-4404, 2012.
- 796 33. **Li X, Jiang J, Zhao X, Wang J, Han H, Zhao Y, Peng B, Zhong R, Ying W, and Qian X.** N-
797 glycoproteome analysis of the secretome of human metastatic hepatocellular carcinoma cell
798 lines combining hydrazide chemistry, HILIC enrichment and mass spectrometry. *PLoS one* 8:
799 e81921, 2013.
- 800 34. **Liu X, Chhipa RR, Nakano I, and Dasgupta B.** The AMPK inhibitor compound C is a
801 potent AMPK-independent antiglioma agent. *Mol Cancer Ther* 13: 596-605, 2014.
- 802 35. **Liu X, Chhipa RR, Pooya S, Wortman M, Yachyshin S, Chow LM, Kumar A, Zhou X,**
803 **Sun Y, Quinn B, McPherson C, Warnick RE, Kendler A, Giri S, Poels J, Norga K, Viollet B,**
804 **Grabowski GA, and Dasgupta B.** Discrete mechanisms of mTOR and cell cycle regulation by
805 AMPK agonists independent of AMPK. *Proceedings of the National Academy of Sciences of*
806 *the United States of America* 111: E435-444, 2014.
- 807 36. **Llovet JM, Montal R, Sia D, and Finn RS.** Molecular therapies and precision medicine
808 for hepatocellular carcinoma. *Nat Rev Clin Oncol* 15: 599-616, 2018.
- 809 37. **Llovet JM, Zucman-Rossi J, Pikarsky E, Sangro B, Schwartz M, Sherman M, and**
810 **Gores G.** Hepatocellular carcinoma. *Nat Rev Dis Primers* 2: 16018, 2016.
- 811 38. **Longato L, Andreola F, Davies SS, Roberts JL, Fusai G, Pinzani M, Moore K, and**
812 **Rombouts K.** Reactive gamma-ketoaldehydes as novel activators of hepatic stellate cells in
813 vitro. *Free radical biology & medicine* 102: 162-173, 2017.
- 814 39. **Marrone G, De Chiara F, Bottcher K, Levi A, Dhar D, Longato L, Mazza G, Zhang Z,**
815 **Marrali M, Iglesias AF, Hall A, Luong TV, Viollet B, Pinzani M, and Rombouts K.** The AMPK-
816 v-ATPase-pH axis: A key regulator of the pro-fibrogenic phenotype of human hepatic stellate
817 cells. *Hepatology* 2018.
- 818 40. **Mazza G, Telesse A, Al-Akkad W, Frenguelli L, Levi A, Marrali M, Longato L,**
819 **Thanapirom K, Vilia MG, Lombardi B, Crowley C, Crawford M, Karsdal MA, Leeming DJ,**
820 **Marrone G, Bottcher K, Robinson B, Del Rio Hernandez A, Tamburrino D, Spoletini G,**
821 **Malago M, Hall AR, Godovac-Zimmermann J, Luong TV, De Coppi P, Pinzani M, and**
822 **Rombouts K.** Cirrhotic Human Liver Extracellular Matrix 3D Scaffolds Promote Smad-
823 Dependent TGF-beta1 Epithelial Mesenchymal Transition. *Cells* 9: 2019.

- 824 41. **Mihaylova MM, and Shaw RJ.** The AMPK signalling pathway coordinates cell growth,
825 autophagy and metabolism. *Nat Cell Biol* 13: 1016-1023, 2011.
- 826 42. **Pinzani M.** Pathophysiology of Liver Fibrosis. *Digestive diseases* 33: 492-497, 2015.
- 827 43. **Piscaglia F, Svegliati-Baroni G, Barchetti A, Pecorelli A, Marinelli S, Tiribelli C,**
828 **Bellentani S, and Group H-NIS.** Clinical patterns of hepatocellular carcinoma in nonalcoholic
829 fatty liver disease: A multicenter prospective study. *Hepatology* 63: 827-838, 2016.
- 830 44. **Qiu SL, Xiao ZC, Piao CM, Xian YL, Jia LX, Qi YF, Han JH, Zhang YY, and Du J.** AMP-
831 activated protein kinase alpha2 protects against liver injury from metastasized tumors via
832 reduced glucose deprivation-induced oxidative stress. *The Journal of biological chemistry*
833 289: 9449-9459, 2014.
- 834 45. **Qu H, and Yang X.** Metformin inhibits angiogenesis induced by interaction of
835 hepatocellular carcinoma with hepatic stellate cells. *Cell Biochem Biophys* 71: 931-936,
836 2015.
- 837 46. **Rattan R, Giri S, Singh AK, and Singh I.** 5-Aminoimidazole-4-carboxamide-1-beta-D-
838 ribofuranoside inhibits cancer cell proliferation in vitro and in vivo via AMP-activated
839 protein kinase. *The Journal of biological chemistry* 280: 39582-39593, 2005.
- 840 47. **Rebouissou S, La Bella T, Rekik S, Imbeaud S, Calatayud AL, Rohr-Udilova N, Martin**
841 **Y, Couchy G, Bioulac-Sage P, Grasl-Kraupp B, de Koning L, Ganne-Carrie N, Nault JC, Ziol M,**
842 **and Zucman-Rossi J.** Proliferation Markers Are Associated with MET Expression in
843 Hepatocellular Carcinoma and Predict Tivantinib Sensitivity In Vitro. *Clinical cancer research*
844 : an official journal of the American Association for Cancer Research 23: 4364-4375, 2017.
- 845 48. **Rombouts K.** Hepatic Stellate Cell Culture Models. In: *Stellate Cells in Health and*
846 *Disease*, edited by Gandhi CRaPMAcademic Press Elsevier, 2015, p. 15-27.
- 847 49. **Rombouts K, and Carloni V.** Determination and Characterization of Tetraspanin-
848 Associated Phosphoinositide-4 Kinases in Primary and Neoplastic Liver Cells. *Methods Mol*
849 *Biol* 1376: 203-212, 2016.
- 850 50. **Ross FA, MacKintosh C, and Hardie DG.** AMP-activated protein kinase: a cellular
851 energy sensor that comes in 12 flavours. *FEBS J* 283: 2987-3001, 2016.
- 852 51. **Saxton RA, and Sabatini DM.** mTOR Signaling in Growth, Metabolism, and Disease.
853 *Cell* 169: 361-371, 2017.
- 854 52. **Short JD, Houston KD, Dere R, Cai SL, Kim J, Johnson CL, Broaddus RR, Shen J,**
855 **Miyamoto S, Tamanoi F, Kwiatkowski D, Mills GB, and Walker CL.** AMP-activated protein
856 kinase signaling results in cytoplasmic sequestration of p27. *Cancer Res* 68: 6496-6506,
857 2008.
- 858 53. **Steinberg GR, and Carling D.** AMP-activated protein kinase: the current landscape
859 for drug development. *Nature reviews Drug discovery* 2019.
- 860 54. **Sun Y, Connors KE, and Yang DQ.** AICAR induces phosphorylation of AMPK in an
861 ATM-dependent, LKB1-independent manner. *Molecular and cellular biochemistry* 306: 239-
862 245, 2007.
- 863 55. **Suter M, Riek U, Tuerk R, Schlattner U, Wallimann T, and Neumann D.** Dissecting
864 the role of 5'-AMP for allosteric stimulation, activation, and deactivation of AMP-activated
865 protein kinase. *The Journal of biological chemistry* 281: 32207-32216, 2006.
- 866 56. **Thorgeirsson SS, and Grisham JW.** Molecular pathogenesis of human hepatocellular
867 carcinoma. *Nat Genet* 31: 339-346, 2002.
- 868 57. **Trautwein C, Friedman SL, Schuppan D, and Pinzani M.** Hepatic fibrosis: Concept to
869 treatment. *Journal of hepatology* 62: S15-24, 2015.

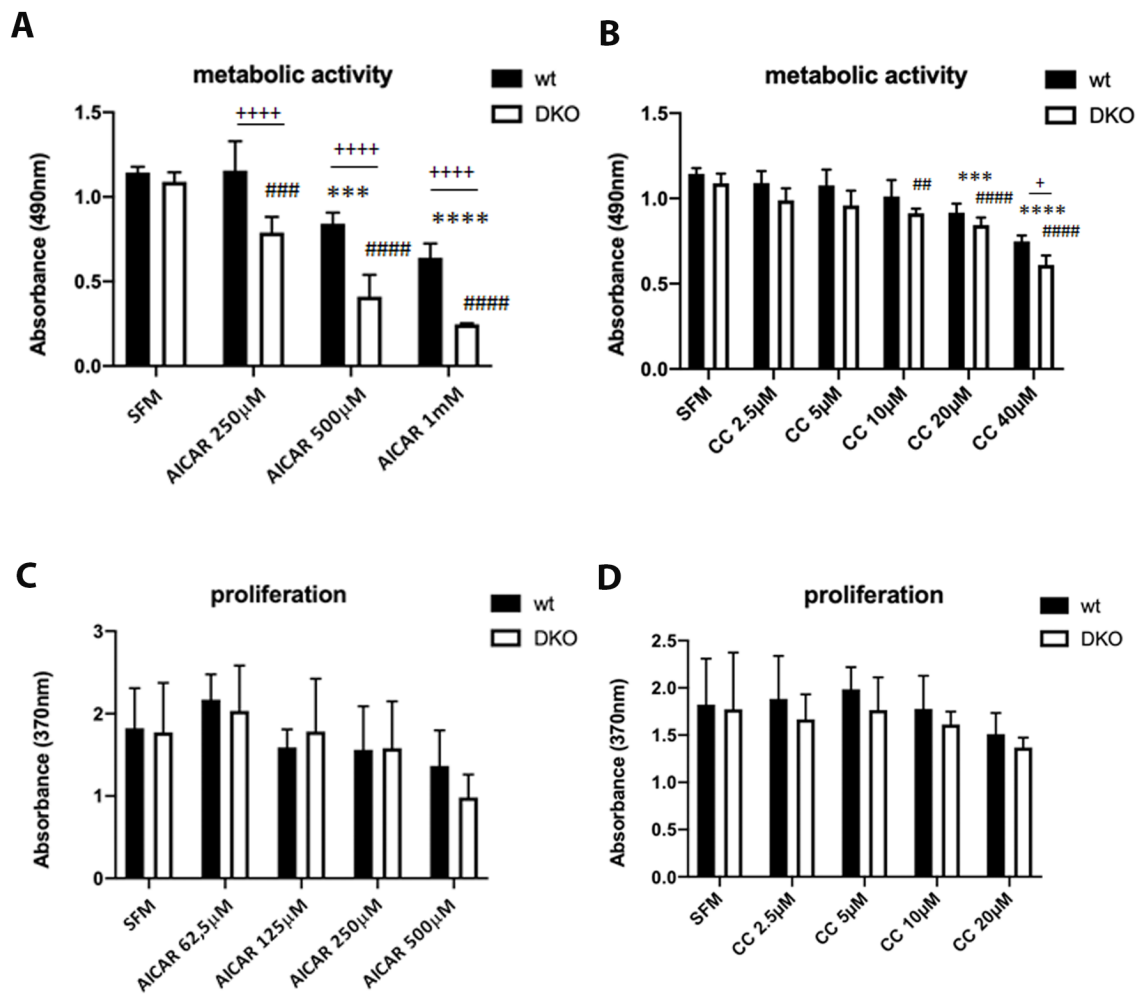
- 870 58. **Uphoff CC, and Drexler HG.** Detection of mycoplasma contaminations in cell cultures
871 by PCR analysis. *Hum Cell* 12: 229-236, 1999.
- 872 59. **Vucicevic L, Misirkic M, Janjetovic K, Harhaji-Trajkovic L, Prica M, Stevanovic D,**
873 **Isenovic E, Sudar E, Sumarac-Dumanovic M, Micic D, and Trajkovic V.** AMP-activated
874 protein kinase-dependent and -independent mechanisms underlying in vitro antiglioma
875 action of compound C. *Biochemical pharmacology* 77: 1684-1693, 2009.
- 876 60. **Vucicevic L, Misirkic M, Janjetovic K, Vilimanovich U, Sudar E, Isenovic E, Prica M,**
877 **Harhaji-Trajkovic L, Kravic-Stevovic T, Bumbasirevic V, and Trajkovic V.** Compound C
878 induces protective autophagy in cancer cells through AMPK inhibition-independent
879 blockade of Akt/mTOR pathway. *Autophagy* 7: 40-50, 2011.
- 880 61. **Woods A, Vertommen D, Neumann D, Turk R, Bayliss J, Schlattner U, Wallimann T,**
881 **Carling D, and Rider MH.** Identification of phosphorylation sites in AMP-activated protein
882 kinase (AMPK) for upstream AMPK kinases and study of their roles by site-directed
883 mutagenesis. *The Journal of biological chemistry* 278: 28434-28442, 2003.
- 884 62. **Xiang Y, Liu Y, Yang Y, Hu H, Hu P, Ren H, and Zhang D.** A secretomic study on
885 human hepatocellular carcinoma multiple drug-resistant cell lines. *Oncol Rep* 34: 1249-1260,
886 2015.
- 887 63. **Yang WL, Perillo W, Liou D, Marambaud P, and Wang P.** AMPK inhibitor compound
888 C suppresses cell proliferation by induction of apoptosis and autophagy in human colorectal
889 cancer cells. *J Surg Oncol* 106: 680-688, 2012.
- 890 64. **Zanieri F, Levi A, Montefusco D, Longato L, De Chiara F, Frenguelli L, Omenetti S,**
891 **Andreola F, Luong TV, Massey V, Caballeria J, Fondevila C, Shanmugavelandy SS, Fox T,**
892 **Mazza G, Argemi J, Bataller R, Cowart LA, Kester M, Pinzani M, and Rombouts K.**
893 Exogenous Liposomal Ceramide-C6 Ameliorates Lipidomic Profile, Energy Homeostasis, and
894 Anti-Oxidant Systems in NASH. *Cells* 9: 2020.
- 895 65. **Zhao P, and Saltiel AR.** From overnutrition to liver injury: AMP-activated protein
896 kinase in nonalcoholic fatty liver diseases. *The Journal of biological chemistry* 295: 12279-
897 12289, 2020.
- 898



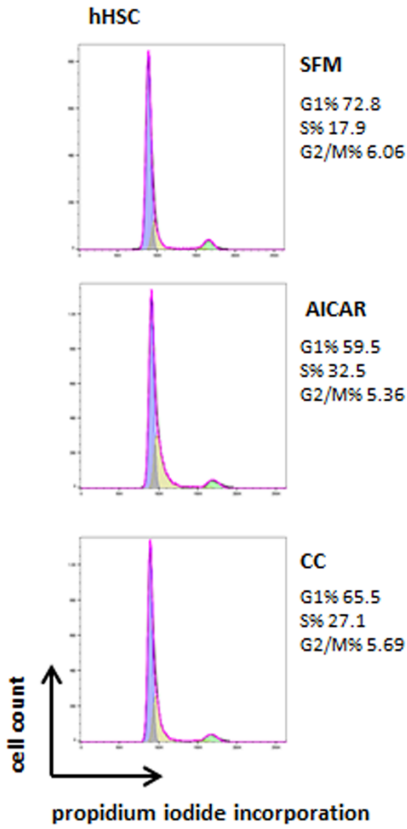
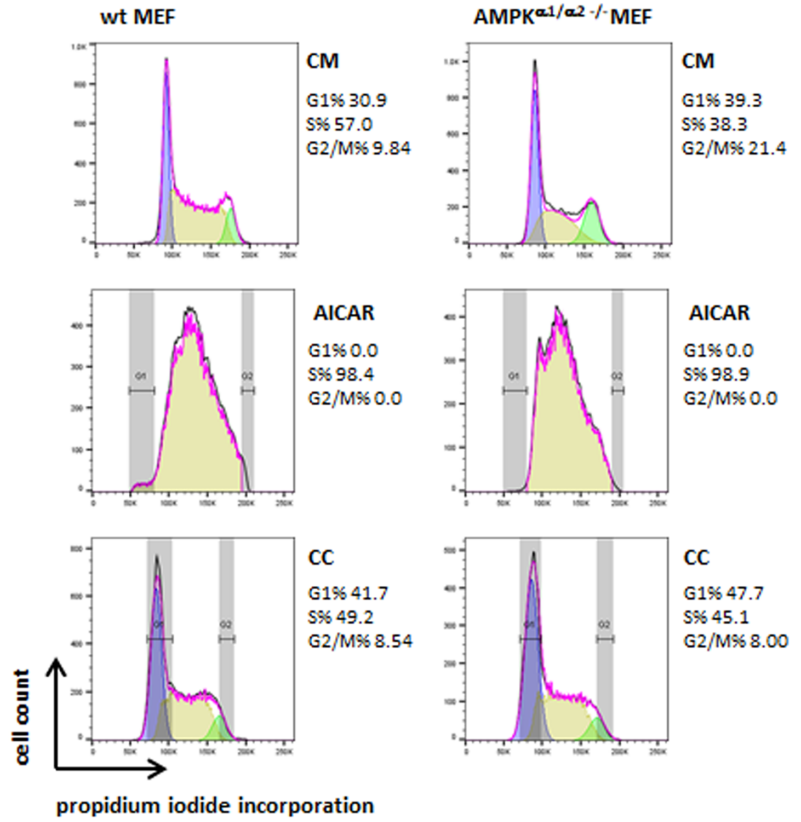
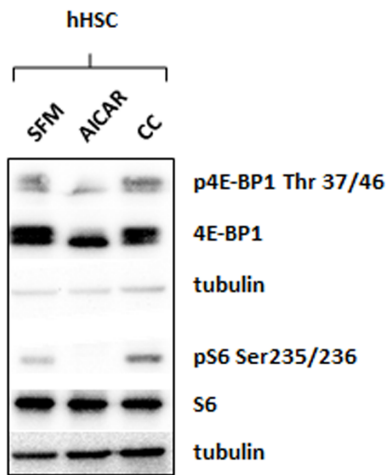
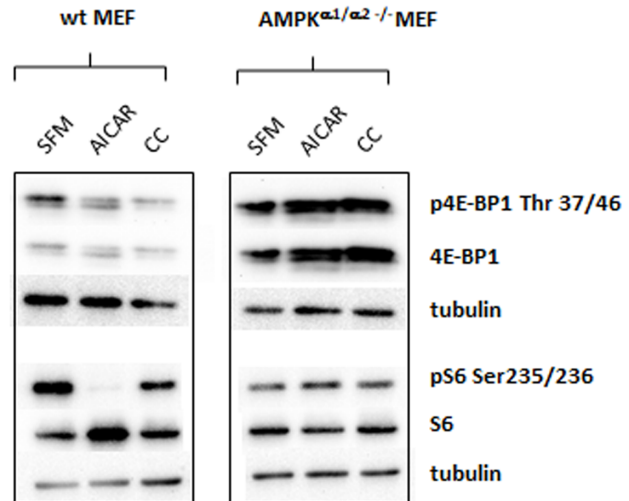
K. Böttcher et al., Figure 1

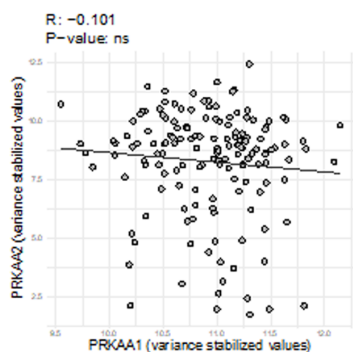
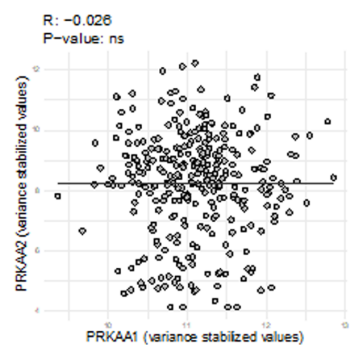
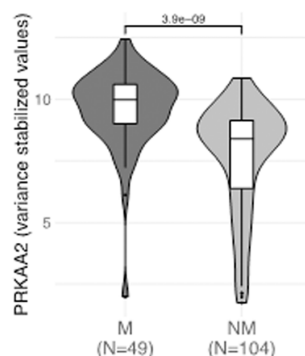
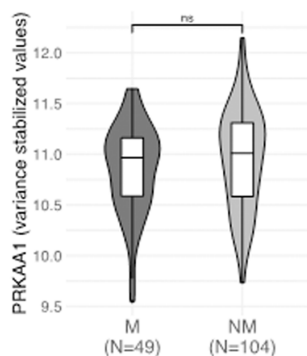
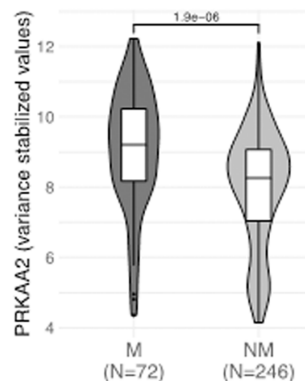
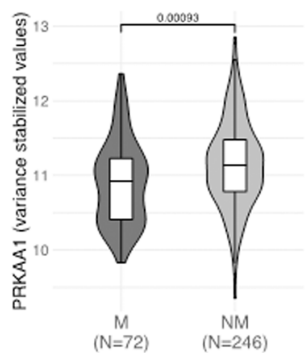
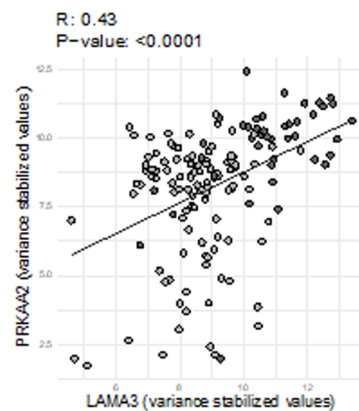
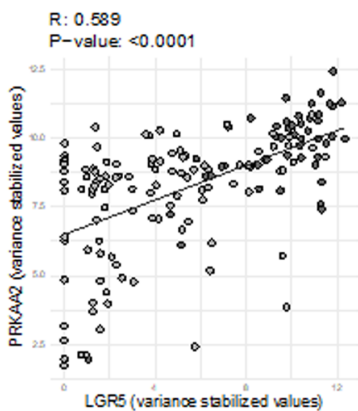
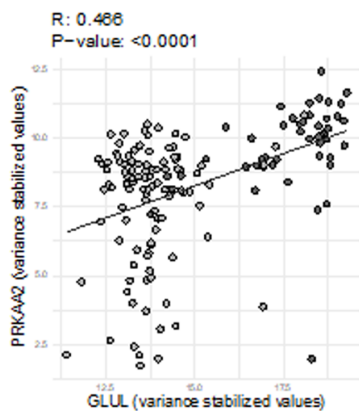


K. Böttcher et al., Figure 2

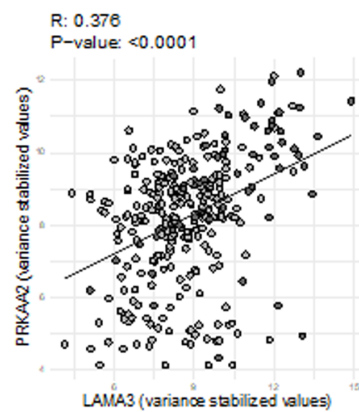
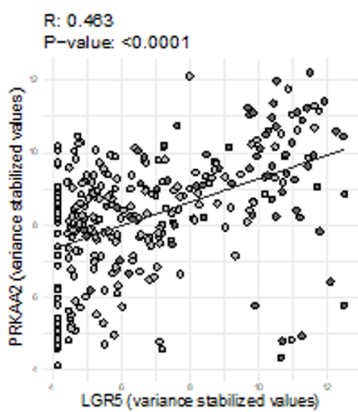
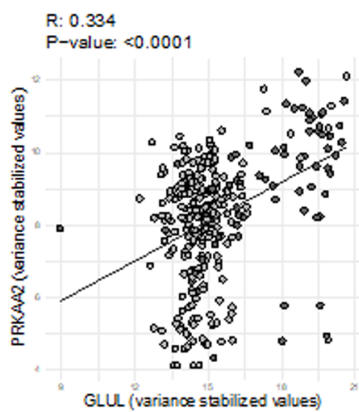


K. Böttcher et al., Figure 3

A**B****C****D**

A**LICA-FR****TCGA****B****LICA-FR****TCGA****CTNNB1****CTNNB1****C****LICA-FR****CTNNB1**

◆ M
◆ NM

TCGA**CTNNB1**

◆ M
◆ NM

